International Immunopharmacology 77 (2019) 105963

Contents lists available at ScienceDirect

International Immunopharmacology

journal homepage: www.elsevier.com/locate/intimp

LXW7 attenuates inflammation via suppressing Akt/nuclear factor kappa B and mitogen-activated protein kinases signaling pathways in lipopolysaccharide-stimulated BV2 microglial cells

Sijia Peng[a], Jingjing Jia[c], Jingjing Sun[a], Qizhi Xie[a], Xiaoyun Zhang[a], Yuanfei Deng[b], Li Yi[a,*]

[a] Department of Neurology, Peking University Shenzhen Hospital, Shenzhen, China
[b] National Clinical Research Center for Geriatric Diseases Shenzhen Center, Peking University Shenzhen Hospital, Shenzhen, China
[c] Department of Neurology, Peking University First Hospital, No.8 Xishiku Street, Xicheng District, Beijing 100034, China

ARTICLE INFO

Keywords:
Integrin inhibitor
LXW7
Inflammation
Microglia
Akt/NF-κB
MAPK

ABSTRACT

Microglia activation is closely linked to ischemia, various chronic neurodegenerative diseases (e.g., Alzheimer's disease, Parkinson's disease, multiple sclerosis, amyotrophic lateral sclerosis), and many other central nervous system diseases. Accumulating evidence suggests that depressing the microglial inflammatory response could be an effective treatment for inflammatory disorders. The integrin αvβ3 inhibitor LXW7 has a neuroprotective effect; however, its anti-inflammatory effects and underlying mechanism remain unclear. Thus, we examined whether LXW7 would inhibit inflammatory cytokines and mediators, and we evaluated the potential mechanisms of its neuroprotective effects. Nitrite analysis revealed LXW7 reduced the nitric oxide (NO) level. Reverse transcription quantitative polymerase chain reaction (RT-qPCR) suggested that LXW7 suppressed the expression of proinflammatory genes for tumor necrosis factor-alpha (TNF-α), interleukin 1-beta (IL-1β), inducible nitric oxide synthase (iNOS), cyclooxygenase 2 (COX-2), and anti-inflammatory gene interleukin 10 (IL-10) at the messenger ribonucleic acid level. Enzyme-linked immunosorbent assay results demonstrated that LXW7 treatment reduced the expression of prostaglandin E2 (PGE2), TNF-α, IL-1β and IL-10 at the protein level. Western blotting was conducted to confirm the upregulation of inflammatory factors, including iNOS and COX-2 at the protein level. LXW7 inhibited major genes in the Akt/NF-κB and c-Jun NH2-terminal kinase/ mitogen-activated protein kinases (JNK/MAPK) signaling pathways. Immunofluorescence revealed that LXW7 inhibited the nuclear translocation of nuclear factor kappa B (NF-κB). Thus, LXW7 effectively alleviated LPS-induced inflammatory damage and had neuroprotective effects. The anti-inflammatory effects of LXW7 may be associated with the inhibition of microglial activation via Akt/NF-κB and JNK/MAPK signaling pathways by blocking integrin αvβ3 receptor. The present study's findings suggest that LXW7 has a substantial therapeutic potential for treating inflammatory and neurodegenerative diseases.

1. Introduction

Microglia cells are a type of resident innate immune cells in the central nervous system (CNS). They provide primary immune monitoring and act as immune defense cells in protective mechanisms. Microglial cells react quickly in response to stress in their environment, whereas chronic microglial activation induced by infection or inflammation leads to microglial overactivation and microglial degeneration [1]. Lipopolysaccharide (LPS)-induced microglial activation is an early and prominent source of a variety of neurotoxic inflammatory cytokines that cause neuronal damage such as interleukin-1 (IL-1β), tumor necrosis factor-α (TNF-α), inducible nitric oxide synthase (iNOS), cyclooxygenase 2 (COX-2), as well as other proinflammatory cytokines [2–4]. The factors that contribute to neurotoxicity are closely linked to many neurodegenerative diseases such as Alzheimer's disease, Parkinson's disease, multiple sclerosis, amyotrophic lateral sclerosis, and neural death [5]. Thus, suppressing these proinflammatory cytokines represents a novel therapeutic approach for treating inflammatory disease. The *cyclo*-Arg-Gly-Asp-D-Phe-Val (*cyclo*-RGDfv) peptide LXW7 has or enhances anti-inflammatory and anti-injury effects in vitro and in vivo [6,7]. LXW7 is an αvβ3 integrin peptide ligand that is used in one-bead one-compound combinatorial technology. LXW7 binds to endothelial progenitor cells/endothelial cells (EPCs/ECs) via αvβ3 integrin to block the binding between αvβ3 and its ligands [8–10]. The

* Corresponding author.
E-mail addresses: dengyf5666@hotmail.com (Y. Deng), yilitj@hotmail.Com (L. Yi).

https://doi.org/10.1016/j.intimp.2019.105963
Received 10 June 2019; Received in revised form 7 September 2019; Accepted 3 October 2019
Available online 13 November 2019

PI3K/Akt signaling pathway regulates the inflammatory response in BV2 microglia [11,12]. Nuclear factor kappa B (NF-κB) is a transcription factor that regulates the expression of the iNOS and COX-2 genes; furthermore, it influences the production of NO and prostaglandin E2 (PGE2) [13]. The mitogen-activated protein kinase (MAPK) signaling pathway also regulates the production of inflammatory factors. The objectives of this study were to examine the inhibitory effect of LXW7 on LPS-stimulated BV2 microglia and to determine whether LXW7 downregulates inflammatory cytokines and modulates microglia phenotypes via Akt/NF-κB and mitogen-activated protein kinases (MAPK) signaling pathways.

2. Materials and methods

2.1. Preparation of LXW7

LXW7 was designed by the Department of Biochemistry and Molecular Medicine at the University of California–Davis (Sacramento, CA, USA). The drug used in the experiment was purchased from Zhejiang Ontores Biotechnologies, Co., Ltd. (lot no.: P151536; Hangzhou, China). The stock solution (100 mg/ml concentration) was produced by dissolving LXW7 in phosphate buffered saline (PBS).

2.2. Cell culture and treatment

The BV2 microglial cell line was obtained from the Cell Resource Center at Peking Union Medical College (which is the headquarters of the National Infrastructure of Cell Line Resource [NSTI]). BV2 cells were cultured in high-glucose Dulbecco's modified Eagle's medium (Gibco, Shanghai, China) supplemented with 10% fetal bovine serum (FBS) (Gibco, South America) and 1% penicillin–streptomycin. The cells were maintained at 37 °C in a humidified atmosphere containing 95% air and 5% carbon dioxide (CO_2). For stimulation, cells were pretreated with LPS to yield a final concentration of 1.0 μg/ml. For reverse transcription quantitative polymerase chain reaction (RT-qPCR) and western blotting, the BV2 microglial cells were seeded in 6-well plates (2×10^5 cells/well). They were then treated with or without LXW7 (1 μmol/L) for 1 h before undergoing treatment with LPS (1.0 μg/ml) for another 24 h. For the enzyme-linked immunosorbent assay (ELISA) and immunofluorescence tests, BV2 microglial cells were seeded in 24-well plates (1×10^5 cells/well) and were treated with or without LXW7 (1 μmol/L) for 1 h before undergoing treatment with LPS (1.0 μg/ml) for another 24 h. For the cell counting kit-8 (CCK-8) assay and nitrite assay, BV2 microglial cells were seeded in 96-well plates (5000 cells/well), and then were treated with or without LXW7 (1 μmol/L) for 1 h before undergoing treatment with LPS (1.0 μg/ml) for another 24 h.

The cells were divided into four groups: (1) the control group, (2) LXW7 alone group, (3) LPS alone group, and (4) LPS + LXW7 group. Dulbecco's modified Eagle's medium, FBS, penicillin–streptomycin (P-S), and other tissue culture reagents were purchased from Gibco-BRL (Grand Island, NY, USA). Lipopolysaccharide was purchased from Sigma (Saint Louis, MO, USA). Antibodies against extracellular signal-regulated kinase (ERK), phospho-ERK (p-ERK), JNK, phospho-JNK (p-JNK), p38, phospho-p38 (p-p38), Akt, phosphor-Akt (p-Akt), NF-κB p65, β-actin, glyceraldehyde 3-phosphate dehydrogenase (GAPDH), histone H3, and horseradish peroxidase (HRP) conjugated goat anti-rabbit immunoglobulins were purchased from Cell Signaling Technology (Beverly, MA, USA). Antibodies against iNOS, COX-2, integrin alpha v, integrin beta3 and goat anti-rabbit IgG H&L (Alexa Fluor 488) were purchased from Abcam (Cambridge, UK). Reverse transcription polymerase quantitative chain reaction (RT-qPCR) reagents were purchased from Takara (Tokyo, Japan). Nuclear and cytoplasmic extraction reagents were purchased from Applygen (Beijing, China). Enhanced chemiluminescence-detecting reagents were purchased from Transgen (Beijing, China). Tumor necrosis factor-alpha and IL-1β ELISA kits were obtained from Multi Sciences (Hang Zhou, China). IL-4 and IL-10 ELISA kits were obtained from Beyotime Biotechnology (Shanghai, China) and a PEG2 ELISA kit was obtained from Bioswamp (Wu Han, China).

2.3. Cell morphological examination

In the cell morphology experiment, BV2 cells were pretreated with LXW7 (1 μmol/L) for 1 h before being treated with LPS (1.0 μg/ml) for 24 h. The image was observed using a phase contrast microscope (DM IRB; Leica, Wetzlar, Germany)

2.4. The CCK-8 assay for cell viability

Cell viability of BV2 microglia after treatment with LXW7 was determined by using a CCK-8 assay. The BV2 cells were plated at a density of 5000 cells/well into a 96-well plate and pretreated for 1 h with varying concentrations of LXW7 (i.e., 0 μg/ml, 0.001 μg/ml, 0.01 μg/ml, 0.1 μg/ml, 1 μg/ml, 10 μg/ml, 100 μg/ml), followed for 24 h by treatment with or without LPS (1.0 μg/ml). The CCK-8 solution (10 μl/well) was added to each well and the formation of formazan was measured at 450 nm with a microplate reader after an additional 4-hour incubation. Wells without BV2 cells were used as the blank control group; wells containing cells and the culture medium were the normal control group; and wells containing cells, drugs, and culture medium were the experimental group. The results were calculated as the percentage of the control group cells after subtracting the blank control group as the background from each sample.

2.5. Nitrite assay

The NO levels were measured by using the Griess reaction. BV2 cells were seeded onto a 96-well plate at a density of 5000 cells/well and pretreated for 1 h with LXW7 (1 μmol/l) before undergoing a 24-hour treatment with LPS (1.0 μg/ml). After 24 h of LPS treatment at 37 °C and 5% CO_2, 100 μl of each culture medium were collected and mixed with an equal volume of Griess reagent. The absorbance was read at the 540-nm wavelength on a microplate reader. The NO concentrations were calculated with reference to a sodium nitrite standard curve generated by using known concentrations.

2.6. Reverse transcription quantitative polymerase chain reaction

Reverse transcription quantitative polymerase chain reaction (RT-qPCR) was used to detect the messenger ribonucleic acid (mRNA) transcription of inflammatory cytokines. BV2 microglial cells, which were seeded in 6-well plates at a density of 2×10^5 cells/well, were pretreated with LXW7 (1 μmol/l) for 1 h, followed by stimulation with LPS (1.0 μg/ml) for 24 h. Total ribonucleic acid (RNA) isolated from BV2 microglial cells using TRIzol reagent (Takara, Tokyo, Japan) was reverse transcribed to complementary deoxyribonucleic acid (cDNA) by using the PrimeScript RT reagent kit (Takara, Tokyo, Japan) with gDNA Eraser (Takara). Quantitative real-time polymerase chain reaction (RT-qPCR) was then conducted using the TB Green Premix Ex TaqII kit (Takara, Tokyo, Japan), based on the manufacturer's instructions, and the Roche LightCycler 96 PCR instrument (Roche, Basel, Switzerland). Primers used for RT-qPCR are listed in Table 1.

2.7. Enzyme-linked immunosorbent assay

To detect the production of TNF-α, IL-1β, IL-4, IL-10 and PGE2, cells were cultured at a concentration of 1×10^5 cells/ml in 24-well plates and pretreated with LXW7 (1 μmol/l) for 1 h before being stimulated with LPS (1 μg/ml) for 24 h. The supernatant was collected and centrifuged at 300*g* for 10 min. The secretion of TNF-α and IL-1β was measured using a commercially available ELISA kit (Multi Sciences). The secretion of IL-4 and IL-10 was measured using a commercially

Table 1
The qPCR primers used in the study.

Gene	Primers
TNF-α	Forward 5′- CCCTCACACTCAGATCATCTTCT -3′
	Reverse 5′- GCTACGACGTGGGCTACAG -3′
IL-1β	Forward 5′- GCAACTGTTCCTGAACTCAACT -3′
	Reverse 5′- ATCTTTTGGGGTCCGTCAACT -3′
iNOS	Forward 5′- GTTCTCAGCCCAACAATACAAGA -3′
	Reverse 5′- GTGGACGGGTCGATGTCAC -3′
COX-2	Forward 5′- CAGTTTATGTTGTCTGTCCA -3′
	Reverse 5′- CCAGCACTTCACCCATCAGT -3
IL-4	Forward 5′- GGTCTCAGCCCCCACCTTGC -3′
	Reverse 5′- CCGTGGTGTTCCTTGTTGCCGT -3
IL-10	Forward 5′- AAGGCCATGAATGAATTTGA -3′
	Reverse 5′- TTCGGAGAGAGGTACAAACG -3
β-actin	Forward 5′- GGCTGTATTCCCCTCCATCG -3′
	Reverse 5′- CCAGTTGGTAACAATGCCATGT -3

COX-2, cyclooxygenase 2; IL-1β, interleukin 1-beta; IL-4, interleukin 4; IL-10, interleukin 10; iNOS, inducible nitric oxide synthase; qPCR, quantitative polymerase chain reaction; TNF-α, tumor necrosis factor-alpha.

available ELISA kit (Beyotime Biotechnology). The secretion of PGE2 was measured using an ELISA kit (Bioswamp), based on the manufacturer's protocols. The absorbance was read at the 450-nm and 630-nm wavelengths by using a microplate reader.

2.8. Western blotting

Western blotting was implemented to explore the expression of iNOS, COX2, integrin αv, integrin β3, p-ERK, ERK, p-JNK, JNK, p-p38, p38, NF-κB, Akt, and p-Akt. Cells were seeded in 6-well plates (2×10^5 cells/well) and pretreated with LXW7 (1 μmol/L) for 1 h before being stimulated with LPS (1 μg/ml) for 24 h. The treated BV2 cells were harvested and washed twice using ice-cold PBS, and then lysed in 200 μl of a radioimmunoprecipitation assay buffer with 1% protease inhibitor and a phosphorylated protease inhibitor. After incubation overnight in a −80 ℃ refrigerator, samples were centrifuged at 12,000*g* for 30 min at 4 ℃. A bicinchoninic acid (BCA) kit was used to measure the concentration of protein. A nuclear and cytoplasmic extraction kit was used to extract cytoplasmic protein and nuclear protein, based on the manufacturer's instructions. An equal amount of protein was separated by 10% sodium dodecyl sulfate-polyacrylamide gel electrophoresis (SDS-PAGE) and transferred to polyvinylidene difluoride (PVDF) membranes. The membranes were then blocked for 1 h with tris-buffered saline + Tween (TBST) containing 5% skim milk at room temperature to prevent nonspecific protein binding. They were also incubated overnight at 4 ℃ with the following primary antibodies: iNOS (1:1000), COX2 (1:2000), integrin αv (1:5000), integrin β3 (1:1000), p-JNK (1:1000), JNK (1:1000), p-ERK1/2 (1:2000), ERK1/2 (1:1000), p-p38 (1:1000), p38 (1:1000), p-Akt (1:2000), Akt (1:1000), NF-κB p65 (1:1000), β-actin (1:1000), histone H (1:2000), and GAPDH (1:1000). After washing three times with TBST, the membranes were incubated with the corresponding anti-rabbit horseradish peroxidase (HRP) immunoglobulin G secondary antibodies (1:2000) for 1 h at room temperature. After washing three times, the bands were visualized by using enhanced chemiluminescence (ECL) reagents and an x-ray machine (5220S; Tanon, Shanghai, China). The densitometric values of the bands were measured using Image J software (National Institutes of Health, Bethesda, MD, USA).

2.9. Immunofluorescence

An immunofluorescence assay was used to detect NF-κB p65 nuclear activation and translocation. BV2 microglial cells (1×10^5 cells/well) were seeded on glass coverslips of 24-well plates and then treated with LXW7 (1 μmol/L) for 1 h before treating with LPS (1 μg/ml) for 24 h. Cells were fixed in 4% paraformaldehyde for 30 min, treated with 0.5% Triton X-100 in goat serum at room temperature for 2 h, and sequentially incubated with anti-NF-κB p65 antibody (1:400) overnight at 4 ℃. They were probed with fluorescein isothiocyanate (FITC)-conjugated goat anti-rabbit IgG (Alexa Fluor 488, CST; Abcam) for 30 min at 37 ℃. The cells were stained with 4′,6-diamidino-2-phenylindole dihydrochloride solution (DAPI:1:1000) for 5 min at room temperature and then washed. Fluorescence staining was examined and photographed by using a fluorescence microscope (BX53; Olympus, Tokyo, Japan).

2.10. Statistical analyses

All data are presented as the mean ± the standard deviation. Statistically significant differences between two groups were determined by using the Student's *t*-test, and statistically significant differences for more than two groups was analyzed by using one-way analysis of variance. A value of $P < 0.05$ was statistically significant. Statistical analysis and graph generation were conducted using Graphpad Prism 6.0 (Graphpad Software, San Diego, CA. USA).

3. Results

3.1. Effects of LXW7 and LPS on BV2 cell viability

The CCK-8 assay was used to detect the cytotoxicity of LXW7 and LPS on BV2 cell viability and to prevent a direct influence of potential cytotoxicity in subsequent experiments. Lipopolysaccharide was used to activate microglia cells. As shown in Fig. 1B, the CCK-8 assay results implied LXW7 alone did not produce any cytotoxicity on BV2 cells at different doses of LXW7, while LXW7 in combination with LPS had the same cytotoxicity on BV2 cells at different concentrations (i.e., 0 μg/ml, 0.001 μg/ml, 0.01 μg/ml, 0.1 μg/ml, 1 μg/ml, 10 μg/ml, and 100 μg/ml). These results implied that a reduction in cell viability induced by LPS could be suppressed by LXW7 to some extent.

3.2. Effects of LPS and LXW7 on morphological changes in BV2 microglial cells

As shown in Fig. 1C, we observed morphological changes such as shorter and fewer branches, and thick round cell bodies in LPS-treated BV2 microglia after the 24-hour stimulation with LPS (1 μg/ml). This finding indicated activation of the microglia, whereas the control group and LXW7 alone group had dendritic shapes with longer distal arborization. The cells in the group pretreated for 1 h with LXW7 (1 μmol/L) before LPS stimulation showed moderate improvement in the retraction of branches and round cell bodies. This LPS stimulation-induced morphological change was significantly inhibited by LXW7 pretreatment.

3.3. Determination of experimental drug concentration

We used RT-qPCR to detect the effects of different concentrations of drugs on TNF-α and IL-1β mRNA expression and to compare the different effects of concentrations of 0.1 μM, 1 μM and 10 μM. In the three administration groups, the 1 μM concentration inhibited IL-1β more strongly than the 0.1 μM and 10 μM concentrations, while the effects of 1 μM and 10 μM did not differ significantly on TNF-α mRNA expression (Fig. 2A). Thus, we chose the concentration of 1 μM for the following experiments.

3.4. Effects of LXW7 on LPS-induced NO and PGE2 production in BV2 cells

We evaluated the effects of LXW7 on NO and PGE2 production in LPS-stimulated BV2 microglia to investigate the role of LXW7 in neuroimmunomodulation of BV2 cells. Cell supernatants were collected, the NO level was assessed using the Griess reaction assay. And PGE2 level was measured using an PGE2 ELISA kit. As shown in Fig. 2B and C,

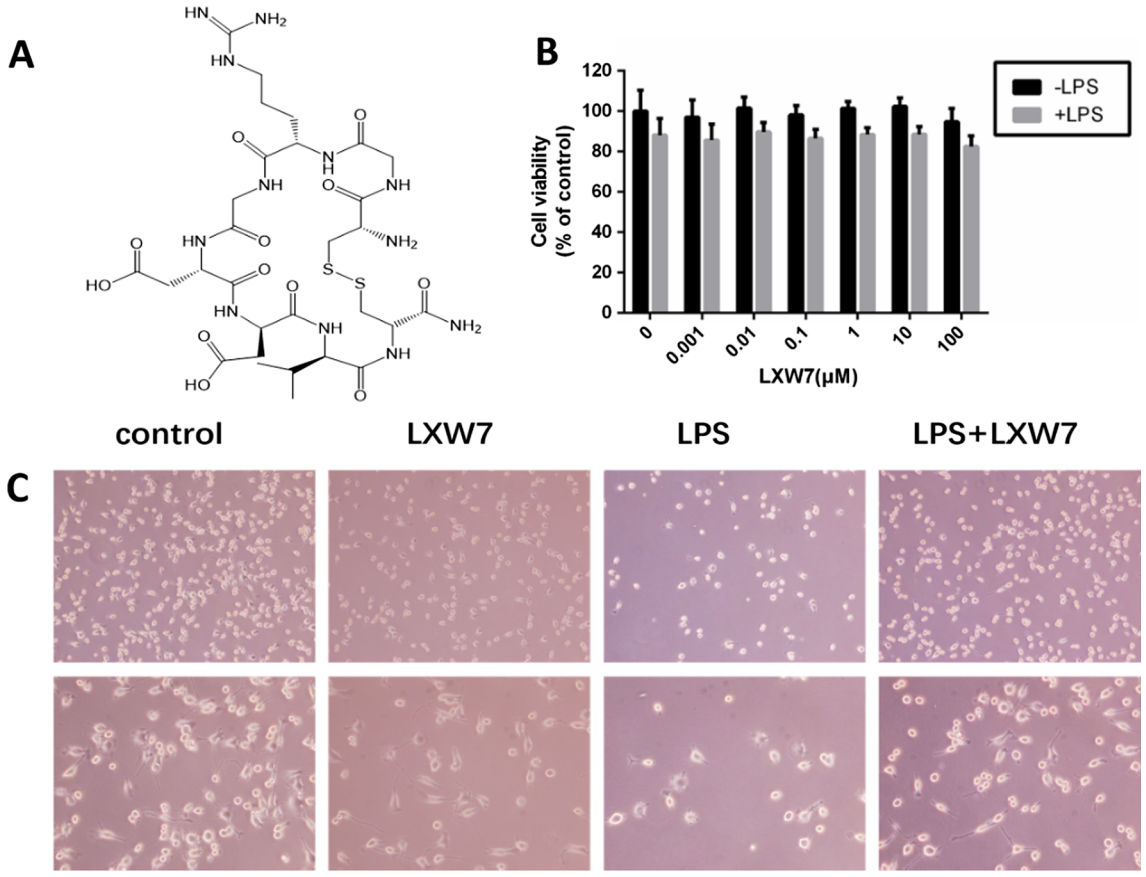

Fig. 1. . (A) The chemical structure of LXW7. (B) The cytotoxicity of BV2 cells with LXW7 alone or with LXW7 in combination with lipopolysaccharide (LPS). Cytotoxicity was determined by using a cell counting kit assay. (C) Morphological changes are visible under a phase contrast microscope (magnification, 100×; upper panel) (magnification, 400×; lower panel). The results are expressed as percentages, relative to the control group. Statistical significance was determined by using one-way analysis of variance. Data are expressed as the mean ± the standard deviation of three independent experiments.

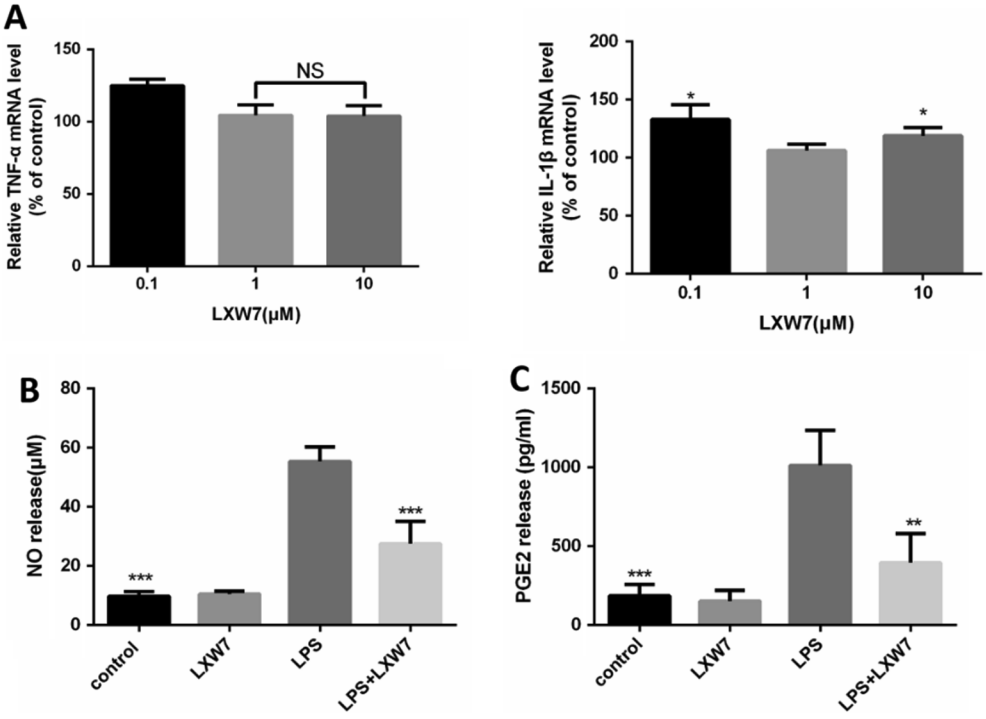

Fig. 2. . (A) The messenger ribonucleic acid expression of TNF-α and IL-1β in lipopolysaccharide (LPS)-stimulated BV2 microglia at concentrations of 0.1 μM, 1 μM and 10 μM. (B) The effects of LXW7 on the production of nitric oxide (NO) in lipopolysaccharide (LPS)-stimulated BV2 microglia. (C) The effects of LXW7 on the production of prostaglandin E2 (PGE2) in lipopolysaccharide (LPS)-stimulated BV2 microglia. Cells were pretreated with LXW7 (1 μg/ml) for 1 h before undergoing LPS treatment for 24 h. The nitric oxide (NO) content of the supernatant was analyzed using an NO assay kit. The amount of PGE2 production was measured by using a PGE2 enzyme-linked immunosorbent assay (ELISA) kit. Data are expressed as the mean ± the standard deviation of three independent experiments. $^{*}P < 0.05$, $^{**}P < 0.01$, and $^{***}P < 0.001$, compared to the LPS group.

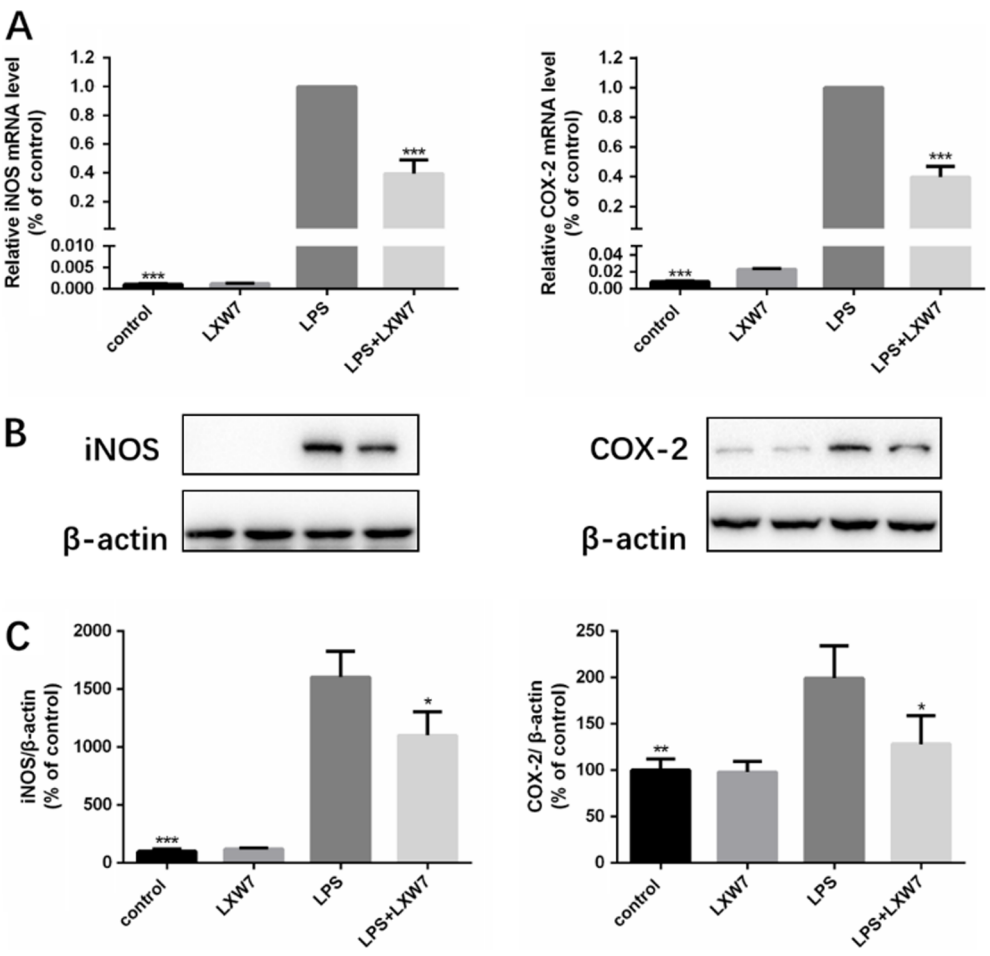

Fig. 3. . The effects of LXW7 on the expression of inducible nitric oxide synthase (iNOS) and cyclooxygenase 2 (COX-2) in BV2 cells. Cells were pretreated with LXW7 for 1 h before undergoing lipopolysaccharide (LPS) treatment for 24 h. (A) The levels of iNOS and COX-2 messenger ribonucleic acid, as assessed using quantitative polymerase chain reaction. (B) The levels of iNOS and COX-2 proteins were assessed by western blot analysis. (C) The semi-quantitative analysis of iNOS and COX-2 proteins. The data in the columns are expressed as the mean ± the standard deviation of three independent experiments. $^{*}P < 0.05$, $^{**}P < 0.01$, and $^{***}P < 0.001$, compared to the LPS group.

the levels of NO and PGE2 were markedly increased after LPS treatment, whereas LXW7 significantly suppressed LPS-induced NO and PGE2 production.

3.5. Effects of LXW7 on LPS-induced iNOS and COX-2 expression in BV2 cells

The LPS-induced production of NO and PGE2 in activated microglia is regulated by their regulatory genes, inducible NO synthase (iNOS) activity, and cyclooxygenase-2 (COX-2) activity. We further examined the effects of LXW7 on the mRNA and protein levels of iNOS and COX-2, based on RT-qPCR and western blot analysis. The RT-qPCR data revealed that LPS-stimulated BV2 cells showed a significant increase in iNOS and COX-2 mRNA expression, compared to the control group and the LXW7 alone group, whereas LXW7 suppressed iNOS and COX-2 expression in LPS-treated BV2 cells (Fig. 3A). The western blot data revealed that LPS-stimulated BV2 cells showed a significant increase in iNOS and COX-2 protein expression, compared to the control group cells and the LXW7 alone group cells, whereas LXW7 suppressed iNOS and COX-2 expression in LPS-treated BV2 cells (Fig. 3B and C). These data suggested that the reduction of iNOS and COX-2 expression at the transcriptional level was correlated with the suppression of iNOS and COX-2 expression at the translation level. The results also suggested that the effects of LXW7 on inhibiting NO and PGE2 production stimulated by LPS treatment had a consistent trend in the reduction in iNOS and COX-2 expression.

3.6. Effects of LXW7 on LPS-induced TNF-α,IL-1β,IL-4 and IL-10 expression in BV2 cells

The RT-qPCR results demonstrated that the production of the cytokines TNF-α, IL-1β, IL-4 and IL-10 was significantly elevated in response to LPS stimulation at the mRNA level. The mRNA expression of TNF-α, IL-1β and IL-10 was dramatically decreased in the LPS + LXW7 group, while the mRNA expression of IL-4 did not differ significantly (Fig. 4A). The ELISA results demonstrated that the upregulation of proinflammatory cytokine TNF-α, IL-1β, IL-4 and IL-10 was significant in the LPS-treated group at protein level. In the LPS + LXW7 group, the level of cytokine proteins (e.g., TNF-α, IL-1β and IL-10) was markedly decreased after LXW7 treatment, while the protein expression of IL-4 did not differ significantly (Fig. 4B). By contrast, the LXW7 alone group had no evident effect on the release of the four proinflammatory cytokines at the mRNA level and the protein level. These data demonstrated that LXW7 has a role in inhibiting TNF-α, IL-1β and IL-10 production in activated BV2 microglia.

3.7. LXW7 reduced MAPKs inflammatory signaling pathway activation in LPS-stimulated BV2 microglia

Mitogen-activated protein kinases signaling has an important role in regulating proinflammatory cytokine production. We examined the protein expressions of p-ERK, ERK, p-JNK, JNK, p-p38, p38, based on western blot analysis, to determine whether the suppressive effect of LXW7 on microglial activation occurred via the MAPK pathway. As shown in Fig. 5, LPS significantly augmented the phosphorylation levels of ERK. JNK, p38 kinases, whereas the total ERK, JNK, and p38 MAPKs expressions did not have an apparent change. Western blotting analysis

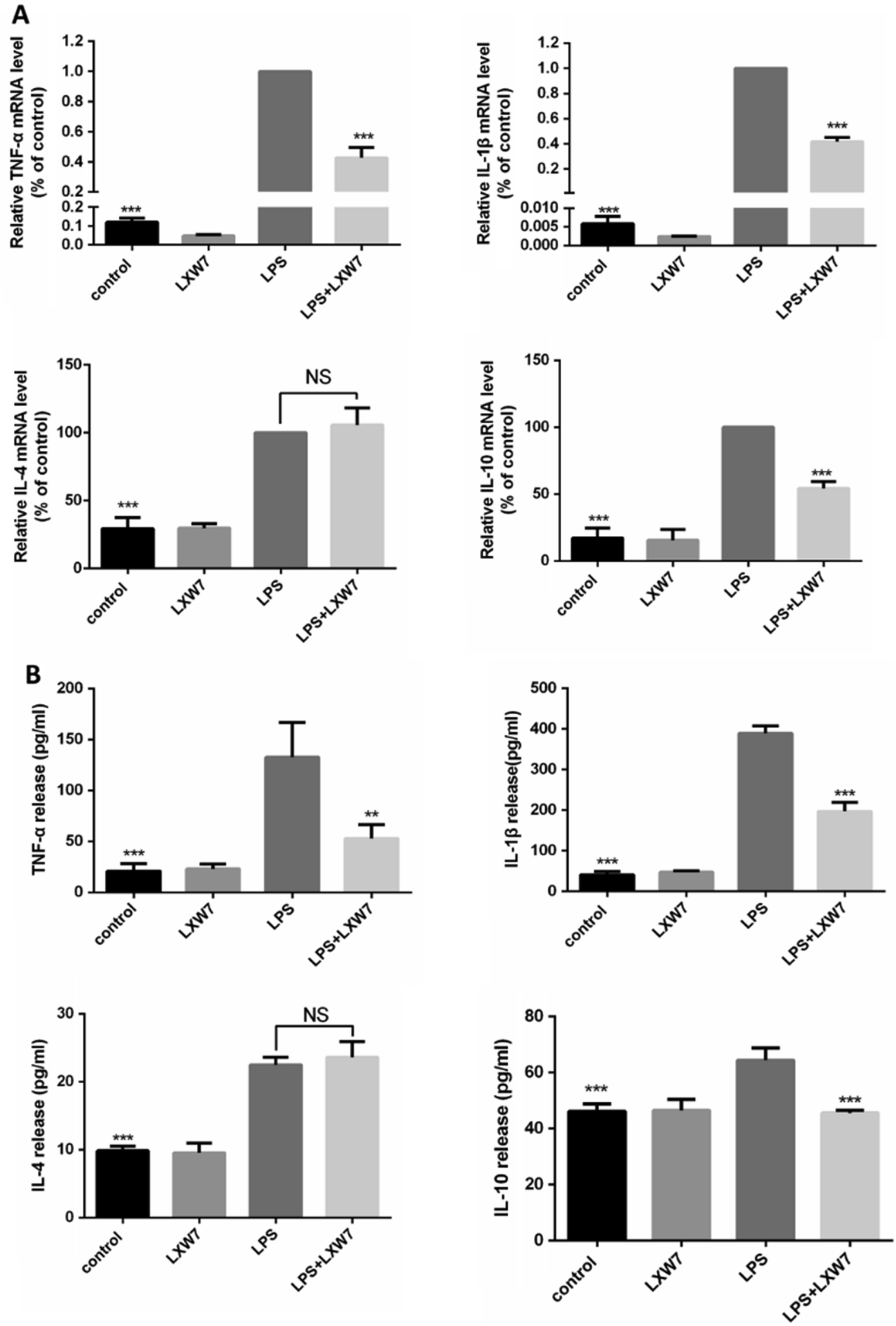

Fig. 4. . The effects of LXW7 on BV2 cells. Cells were pretreated with LXW7 for 1 h before undergoing LPS treatment for 24 h. (A) The levels of tumor necrosis factor-alpha (TNF-α) , interleukin-1β (IL-1β), interleukin-4 (IL-4) and interleukin-10 (IL-10) messenger ribonucleic acid were assessed using quantitative polymerase chain reaction (qPCR). (B) The levels of TNF-α, IL-1β, IL-4 and IL-10 proteins were assessed using a TNF-α enzyme-linked immunosorbent assay (ELISA) kit, an IL-1β ELISA kit, an IL-4 ELISA kit and an IL-10 ELISA kit respectively. Data are expressed as the mean ± the standard deviations of three independent experiments. $^{*}P < 0.05$, $^{**}P < 0.01$, and $^{***}P < 0.001$, compared to the LPS group.

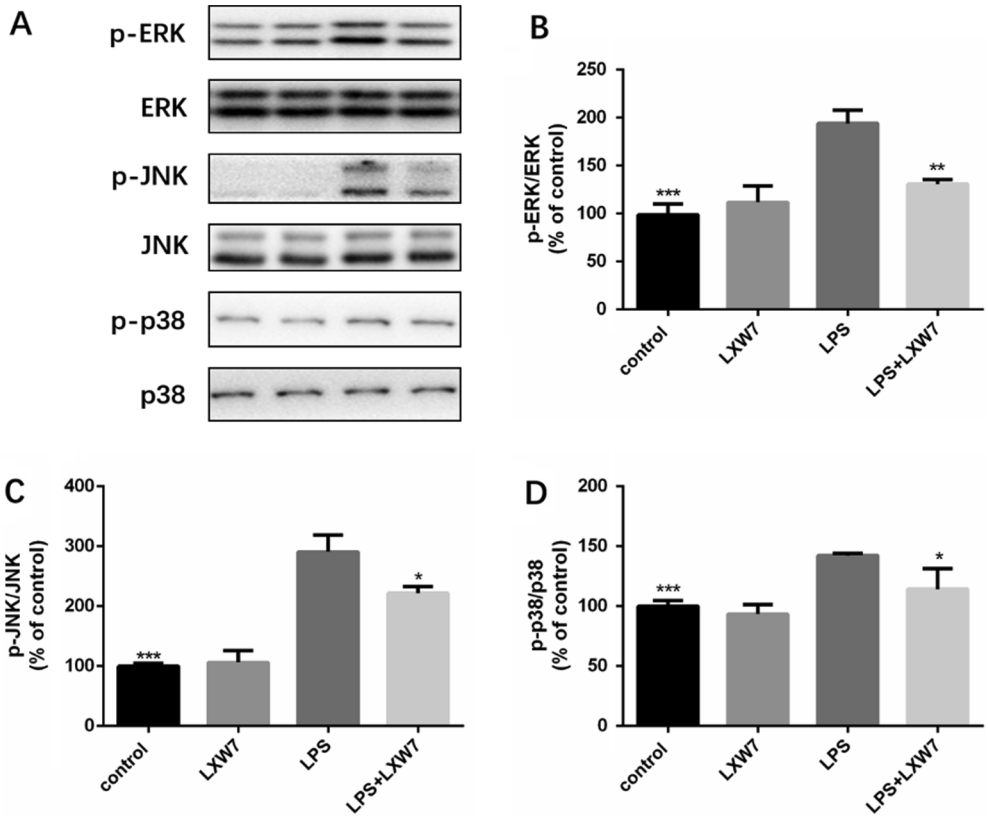

Fig. 5. . The effects of LXW7 on mitogen-activated protein kinase (MAPK) inflammatory signaling pathways in lipopolysaccharide (LPS)-induced BV2 cells. Cells were pretreated with LXW7 for 1 h before undergoing LPS stimulation for 24 h, and then evaluated using western blot. (A) The expression of extracellular signal-regulated kinase (ERK), phospho-ERK (p-ERK), c-Jun NH2-terminal kinase (JNK), phospho-JNK (p-JNK), and p38 and phosp-p38 (p-p38) proteins. (B–D) Semi-quantitative analysis of the proteins. The data in the columns represent the mean ± the standard deviation (SD) of three independent experiments. $^{*}P < 0.05$, $^{**}P < 0.01$, and $^{***}P < 0.001$, compared to the LPS group.

showed reduced expression of p-ERK, p-JNK, and p-p38, after LXW7 treatment. These phenomena indicated that ERK, JNK, and p38 may be targets for the anti-inflammation mechanism of action.

3.8. LXW7 inhibited Akt/NF-κB inflammatory signaling pathway activation and NF-κB translocation in LPS-stimulated BV2 microglia

The NF-κB inflammatory pathway is associated with the modulation of the production of many proinflammatory cytokines. We examined the expression of total proteins and phosphorylated Akt proteins and the expression of NF-κB in the nucleus and in the cytosol by using western blot analysis to detect the activation of Akt/NF-κB inflammatory signaling pathways. We also investigated translocation from the cytoplasm to the nucleus by using immunofluorescence to determine NF-κB translocation in activated BV2 microglia. As shown in Fig. 6, LPS enhanced the phosphorylation of Akt, whereas LXW7 could reduce this effect to some extent. As shown in Figs. 6 and 7, LPS resulted in NF-κB p65 translocation from the cytoplasm to the nucleus and activated the NF-κB inflammatory pathway in BV2 microglia, whereas LXW7 partially reversed the phenomenon, based on the western blot and immunofluorescence results. These findings suggested that LXW7 had an inhibitory effect on LPS-induced inflammatory activities via suppressing Akt/NF-κB inflammatory signaling.

3.9. Effects of LXW7 on integrin αv and β3 in LPS-induced BV2 cells

As shown in Fig. 8, the expression levels of integrin αv and β3 protein increased after LPS treatment compared to the levels in the control group, whereas LXW7 suppressed αv and β3 expression in LPS-treated BV2 cells. We observed no significant change in the expression of integrin αv and β3 in the control group compared with the LXW7 alone group. It is suggested that LXW7 could significantly reduce the expression of integrin αv and β3 in BV2 cells induced by LPS. (see Fig. 9).

4. Discussion

Our study's goal was to determine whether LXW7 inhibits proinflammatory cytokines and mediators released from activated BV2 microglia, which is associated with a variety of CNS diseases. We found that LXW7 was suitable for reducing the proinflammatory mediators NO and PGE2, the proinflammatory cytokines IL-1β and TNF-α and anti-inflammatory cytokine IL-10, which have key roles in various neurodegenerative diseases, but without any cytotoxic effect on microglia. LXW7 also inhibited the production of iNOS, COX-2 and integrin αvβ3 in LPS-stimulated BV2 cells. In addition, LXW7 can regulate the production of proinflammatory cytokines and mediators via adjusting the activation of Akt/NF-κB and MAPK signaling pathway activities.

Microglial cells are brain immune macrophages in the central nervous system which serves crucial functions in many CNS diseases. Activated microglia participate in many inflammation-mediated neurodegenerative diseases such as Alzheimer's disease, Parkinson's disease, amyotrophic lateral sclerosis, multiple sclerosis, and a growing number of other nervous system pathologies [5,14]. Therefore, regulating microglial activation and the production of proinflammatory cytokines and mediators is an effective treatment strategy in many other CNS diseases. Amyloid-beta (Aβ), cytokines, LPS, or interferon-gamma (IFN-γ) are used to activate microglial cells. Lipopolysaccharides are the most common stimulant used in vitro studies [15]. Lipopolysaccharide-stimulated microglial BV2 cells secrete some proinflammatory and neurotoxic cytokines and anti-inflammatory cytokines such as NO, PGE2, TNF-α, IL-1β, IL-4 and IL-10 [16–18]. The release of TNF-α has an important role in microglia activation, neuronal apoptosis, and leukocyte infiltration [19]. Interleukin-1β is responsible for increased permeability of the blood-brain barrier and a decline in tissue function [20]. Interleukin-4 and Interleukin-10 induce an "alternatively activated" phenotype that possesses neuroprotective properties [21,22]. Nitric oxide, an important messenger molecule, is usually produced in LPS-stimulated or IFN-γ-stimulated microglia and has a

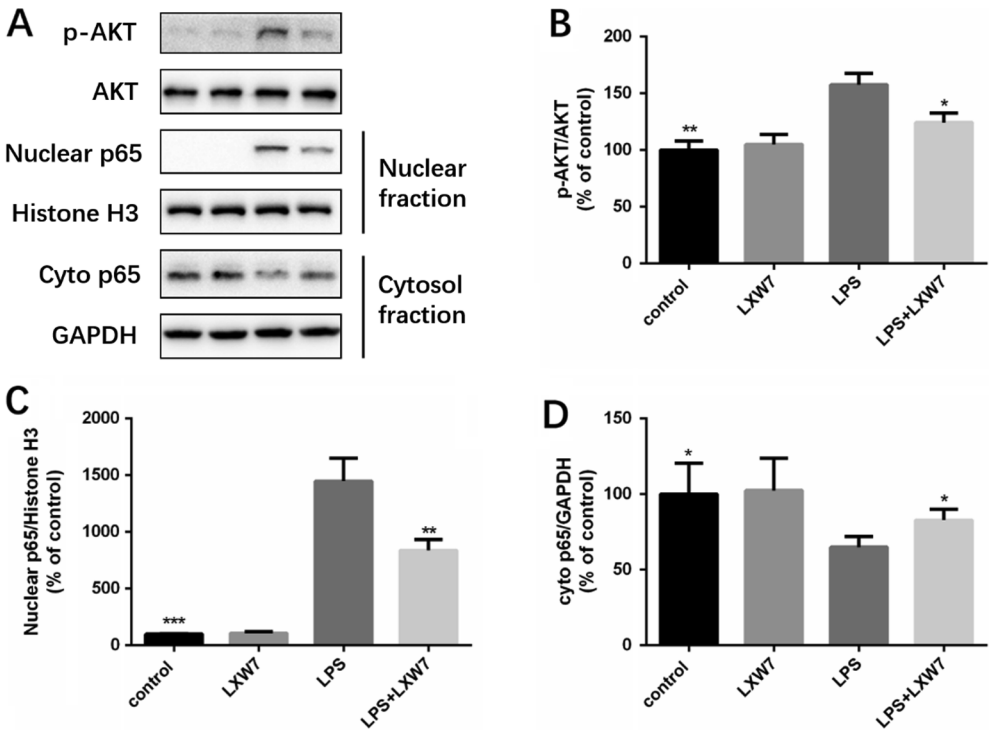

Fig. 6. . The effects of LXW7 on Akt/NF-κB inflammatory signaling pathways in LPS-induced BV2 cells. Cells were pretreated with LXW7 1 h before LPS stimulation for 24 h and then evaluated by using western blot. (A) The expression of Akt, phospho-Akt (p-Akt), nuclear p65, histone H3, cyto p65, and glyceraldehyde 3-phosphate dehydrogenase (GAPDH) proteins. Histone H3 and GAPDH are the internal controls for the nucleus and cytoplasm. (B-D) Semi-quantitative analysis of the proteins. The data in the columns represent the mean ± the standard deviation of three independent experiments. $^{*}P < 0.05$, $^{**}P < 0.01$, and $^{***}P < 0.001$, compared to the LPS group.

pivotal role in vasodilation, neural intercellular signaling communication, host defense, apoptosis, and tissue remodeling [23,24]. Prostaglandin (PG) E2 (PGE2) is a mediator in inflammation and is derived from its precursor arachidonic acid, which also generates PGH2, PGE2, PGD2, PGI2, and PGF2a, and the thromboxane TXA2 [25]. Nitric oxide is primarily produced from l-arginine through the actions of inducible nitric oxide synthase (iNOS), and PGE2 is derived from arachidonic acid through the actions of COX-2. COX enzymes exist two forms: COX1 and COX2. The COX1 form is a constitutively expressed enzyme and has general basic functions, whereas the COX-2 enzyme is associated with many inflammatory activities [26]. Inducible nitric oxide synthase and COX2 are potential therapeutic targets for the treatment of inflammation. Inhibiting iNOS and COX2 reduces neurodegeneration and inhibits inflammation [27,28].

Activated microglia also undergo morphological changes after LPS stimulation [29]. Acute microglia activation after prolonged in vitro LPS exposure (i.e., 72 h) showed a potentially neuroprotective effect, whereas chronic activation of microglia after a short in vitro exposure to LPS (i.e., 24 h) showed strong proinflammatory and neurotoxic effects [30].

Microglia polarization after activation contains two major phenotypes. The classical M1 microglia release inflammatory and cytotoxic

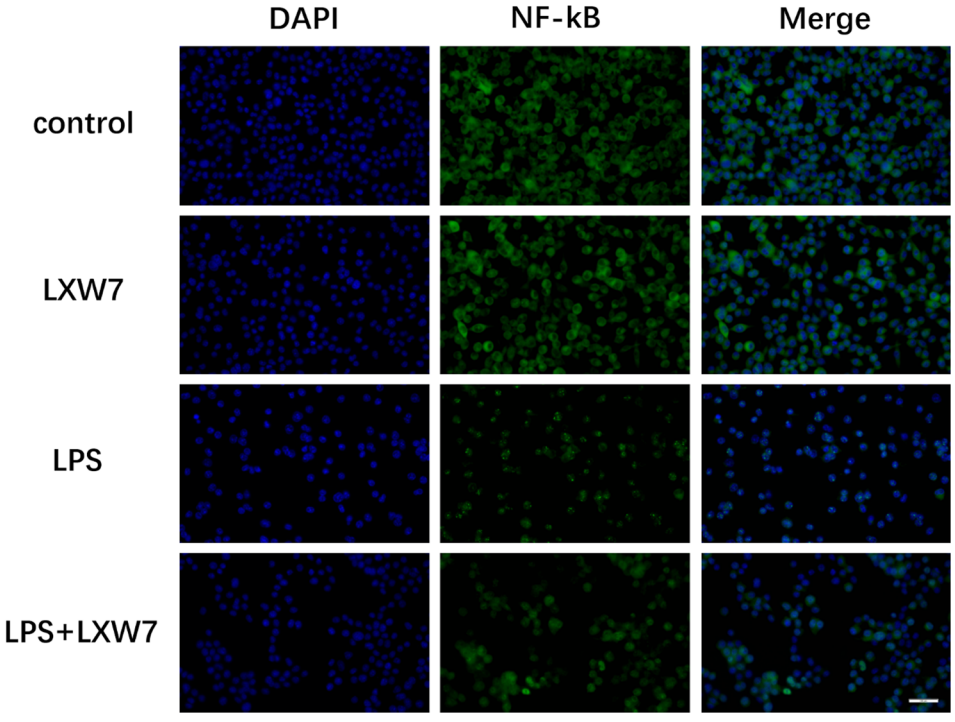

Fig. 7. . The effects of LXW7 on nuclear factor kappa beta (NF-κB) activity in lipopolysaccharide (LPS)-stimulated BV2 microglial cells. Cells were pretreated with LXW7 (1 μg/ml) for 1 h before undergoing LPS treatment for 24 h. The location of NF-κB p65 translocation was detected by using fluorescence microscopy (the scale bar = 100 μm). All experiments were repeated three times, one of which is presented.

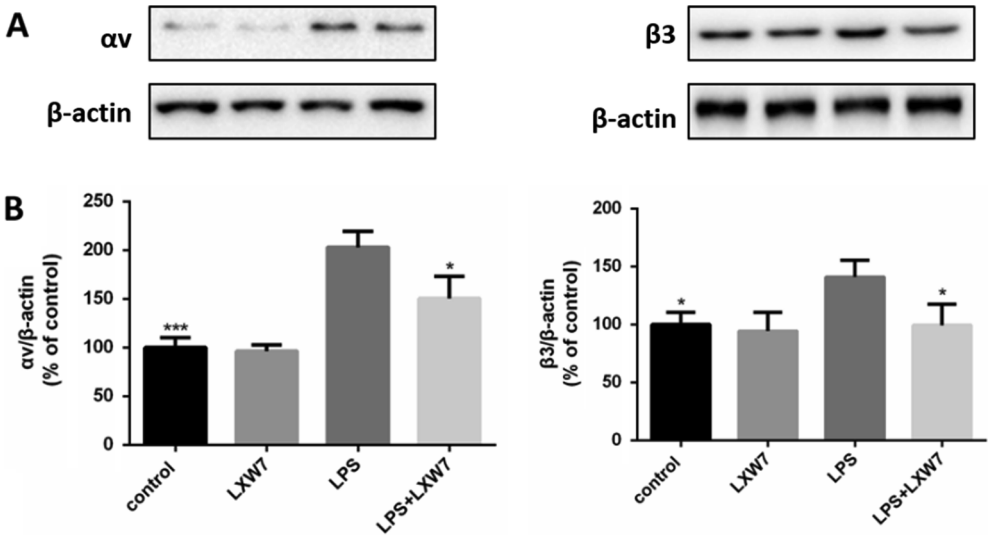

Fig. 8. . The effects of LXW7 on the expression of integrin αv and β3 in BV2 cells. Cells were pretreated with LXW7 for 1 h before undergoing lipopolysaccharide (LPS) treatment for 24 h. (A) The levels of integrin αv and β3 proteins were assessed by western blot analysis. (B) The semi-quantitative analysis of integrin αv and β3 proteins. The data in the columns are expressed as the mean ± the standard deviation of three independent experiments. $^{*}P < 0.05$, $^{**}P < 0.01$, and $^{***}P < 0.001$, compared to the LPS group.

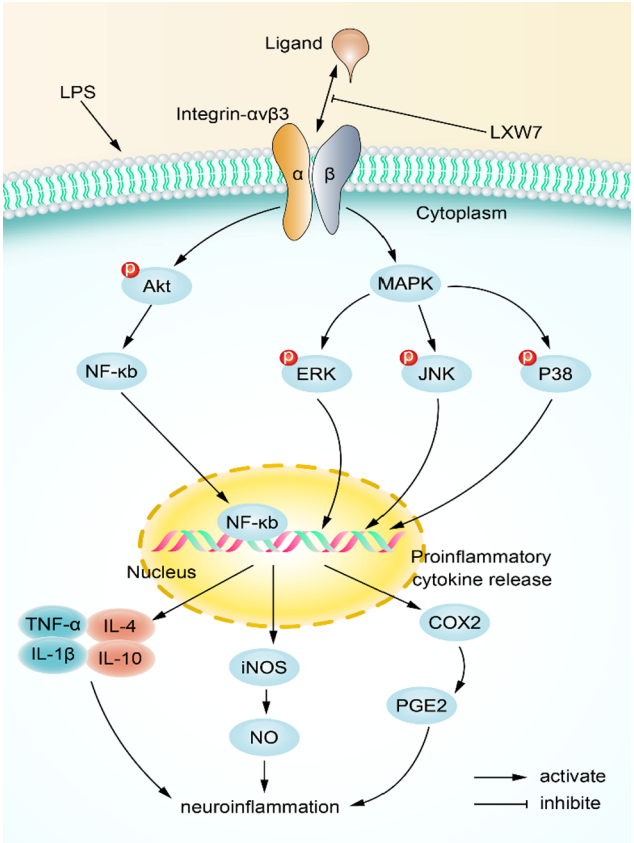

Fig. 9. . The proposed signaling mechanism for the effects of LXW7 on lipopolysaccharide (LPS)-stimulated inflammation in BV2 microglial cells.

factors such as TNF-α and IL-1β, whereas M2 microglia produce anti-inflammatory cytokines such as IL-4, IL-10, and TNF-β [1,31–33].

We then evaluated the expression of proinflammatory factors such as TNF-α, IL-1β, NO, PGE2, iNOS, and COX-2 and anti-inflammatory cytokines such as IL-4 and IL-10. In our study, LXW7 inhibited the LPS-induced overexpression of inflammatory cytokines and mediators mentioned previously. Cytotoxicity was also examined in our study in subsequent experiments Previous studies have proven that NF-κB is an important upstream modulator of multiple inflammatory factors such as TNF-α, IL-1β, iNOS, and COX-2, and is associated with M1 polarization [34–36]. Under normal conditions, NF-κB is in the cytosol as a complex with p50, p60, and IκB subunits. After stimulation by LPS, IκB is degraded and p50 and p60 migrate from the cytosol to the nucleus; the transcription of inflammatory genes is then promoted [37,38]. The inhibition of NFκB-mediated microglial activation attenuates neuronal damage and rescues memory impairment in vitro and in vivo [39–41]. The kinases ERK, JNK, and p38 are members of MAPKs, which are important in signal transduction and in regulating cellular responses such as inflammation, apoptosis, proliferation, and differentiation [42]. Some evidence indicates hyperphosphorylation of MAPK molecules has an effect on NF-κB activation and the subsequent production of inflammatory factors [43]. In addition, several other studies [44–46] have reported that the inhibition of MAPK pathways has a therapeutic effect on the process of inflammatory responses. In this study, we investigated the Akt/NF-κB and MAPKs signaling pathways and found that LPS upregulated the phosphorylation levels of Akt, ERK, JNK, and p38 kinases in BV2 cells. Pretreatment with LXW7 markedly reduced the phosphorylation level of Akt and ERK, JNK, and p38 kinases. Similar to the aforementioned findings, our study revealed that LXW7 could also suppress the nuclear translocation of NFκB, which was induced by LPS stimulation.

LXW7, an αvβ3 integrin cyclic RGD peptide that can specifically target integrin αvβ3, binds to endothelial progenitor cells/endothelial cells (EPCs/ECs) via αvβ3 integrin to block the binding between αvβ3 and its ligands [8–10]. Previous studies have shown that LXW7 has anti-inflammatory and anti-injury effects in vitro and in vivo [6,7]. Our study shows that blocking integrin αvβ3 reduced inflammation by inhibiting the production of proinflammatory cytokines and deactivating the Akt/NF-κB and MAPKs signaling pathway. It is suggested that LXW7 can weaken inflammatory and neurodegenerative damage by regulating integrin signaling.

5. Conclusions

This study demonstrated that the Akt/NF-κB and MAPK signaling pathways may participate in the release of inflammatory cytokines and mediators in LPS-stimulated microglia. LXW7 may have an enhanced neuroprotective role by suppressing the release of inflammatory cytokines and mediators by blocking Akt/NF-κB and MAPK signaling pathways in vitro. Our findings suggested that LXW7 may provide a beneficial effect for treating inflammatory and neurodegenerative damage and may prevent further nerve damage induced by microglial activation.

However, our study has some limitations. One limitation is that LXW7 also inhibits NF-κB activation through another signaling pathway because Akt is just one upstream signaling molecule that activates NF-

κB. Which signaling pathway has the predominant role or has an earlier effect is unclear because the interlaced relationship between two signaling pathways is ambiguous. One limitation is we only examined the effects of LXW7 via Akt/NF-κB and MAPK signaling pathways which have proinflammatory effects. In the future, we should further study the effects of LXW7 via anti-neuroinflammation signaling pathways such as Nrf2/HO-1 signaling pathway. The other limitation is we only examined LXW7 exhibiting its activity by blocking integrin αvβ3 receptor. More studies are needed to substantiate the mechanism LXW7 enters inside BV2 cells.

Acknowledgements

This study was funded by Sanming Project of Medicine in Shenzhen [grant no. SZSM201812096].

Declaration of competing interest

The authors declared that there is no conflict of interest.

Appendix A. Supplementary material

Supplementary data to this article can be found online at https://doi.org/10.1016/j.intimp.2019.105963.

References

[1] M. Czeh, P. Gressens, A.M. Kaindl, The yin and yang of microglia, Dev. Neurosci. 33 (3-4) (2011) 199–209.
[2] U.K. Hanisch, Microglia as a source and target of cytokines, Glia. 40 (2002) 140–155.
[3] R.L. Hunter, N. Dragicevic, K. Seifert, D.Y. Choi, M. Liu, H.C. Kim, W.A. Cass, P.G. Sullivan, G. Bing, Inflammation induces mitochondrial dysfunction and dopaminergic neurodegeneration in the nigrostriatal system, J. Neurochem. 100 (2007) 1375–1386.
[4] C.M. Jeon, I.S. Shin, N.R. Shin, J.M. Hong, O.K. Kwon, H.S. Kim, S.R. Oh, P.K. Myung, K.S. Ahn, *Siegesbeckia glabrescens* attenuates allergic airway inflammation in LPS-stimulated RAW 264.7 cells and OVA induced asthma murine model, Int. Immunopharmacol. 22 (2014) 414–419.
[5] C.K. Glass, K. Saijo, B. Winner, M.C. Marchetto, F.H. Gage, Mechanisms underlying inflammation in neurodegeneration, Cell 140 (2010) 918–934.
[6] J. Jia, T. Zhang, J. Chi, X. Liu, J. Sun, Q. Xie, S. Peng, C. Li, L. Yi, Neuroprotective effect of CeO_2@PAA-LXW7 against H_2O_2-induced cytotoxicity in NGF-differentiated PC12 cells, Neurochem. Res. 43 (2018) 1439–1453.
[7] T. Fang, D. Zhou, L. Lu, X. Tong, J. Wu, L. Yi, LXW7 ameliorates focal cerebral ischemia injury and attenuates inflammatory responses in activated microglia in rats, Braz. J. Med. Biol. Res. 49 (2016) e5287.
[8] Y. Wang, W. Xiao, Y. Zhang, L. Meza, H. Tseng, Y. Takada, J.B. Ames, K.S. Lam, Optimization of RGD-containing cyclic peptides against αvβ3 integrin, Mol. Cancer Ther. 15 (2016) 232–240.
[9] D. Hao, W. Xiao, R. Liu, P. Kumar, Y. Li, P. Zhou, F. Guo, D.L. Farmer, K.S. Lam, F. Wang, A. Wang, Discovery and characterization of a potent and specific peptide ligand targeting endothelial progenitor cells and endothelial cells for tissue regeneration, ACS Chem. Biol. 12 (2017) 1075–1086.
[10] W. Xiao, Y. Wang, E.Y. Lau, J. Luo, N. Yao, C. Shi, L. Meza, H. Tseng, Y. Maeda, P. Kumaresan, R. Liu, F.C. Lightstone, Y. Takada, I.T.S. Lam, The use of one-bead one-compound combinatorial library technology to discover high-affinity αvβ3 integrin and cancer targeting arginine-glycine-aspartic acid ligands with a built-in handle, Mol. Cancer Ther. 9 (2010) 2714–2723.
[11] D.S. Lee, G.S. Jeong, Butein provides neuroprotective and anti-inflammatory effects through Nrf2/ARE-dependent haem oxygenase 1 expression by activating the PI3K/Akt pathway, Br. J. Pharmacol. 173 (2016) 2894–2909.
[12] M.H. Han, W.S. Lee, A. Nagappan, S.H. Hong, J.H. Jung, C. Park, H.J. Kim, G.Y. Kim, G. Kim, J.M. Jung, C.H. Ryu, S.C. Shin, S.C. Hong, Y.H. Choi, Flavonoids isolated from flowers of *Lonicera japonica* Thunb, inhibit inflammatory responses in BV2 microglial cells by suppressing TNF-α and IL-β through PI3K/Akt/NF-κB signaling pathways, Phytother. Res. 30 (2016) 1824–1832.
[13] M.G. Dilshara, K.T. Lee, Y.H. Choi, D.O. Moon, H.J. Lee, S.G. Yun, G.Y. Kim, Potential chemoprevention of LPS-stimulated nitric oxide and prostaglandin E2 production by α-L-rhamnopyranosyl-(1→6)-β-D-glucopyranosyl-3-indolecarbonate in BV2 microglial cells through suppression of the ROS/PI3K/Akt/NF-κB pathway, Neurochem. Int. 67 (2014) 39–45.
[14] B. Liu, J.S. Hong, Role of Microglia in inflammation-mediated neurodegenerative diseases: mechanisms and strategies for therapeutic intervention, J. Pharmacol. Exp. Ther. 304 (2003) 1–7.
[15] U.K. Hanisch, H. Kettenmann, Microglia: active sensor and versatile effector cells in the normal and pathologic brain, Nat. Neurosci. 10 (2007) 1387–1394.
[16] H. Akiyama, S. Barger, S. Barnum, B. Bradt, J. Bauer, G.M. Cole, N.R. Cooper, P. Eikelenboom, M. Emmerling, B.L. Fiebich, C.E. Finch, S. Frautschy, W.S. Griffin, H. Hampel, M. Hull, G. Landreth, L. Lue, R. Mrak, I.R. Mackenzie, P.L. McGeer, M.K. O'Banion, J. Pachter, G. Pasinetti, C. Plata-Salaman, J. Rogers, R. Rydel, Y. Shen, W. Streit, R. Strohmeyer, I. Tooyoma, F.L. Van Muiswinkel, R. Veerhuis, D. Walker, S. Webster, B. Wegrzyniak, G. Wenk, T. Wyss-Coray, Inflammation and Alzheimer's disease, Neurobiol. Aging. 21 (2000) 383–421.
[17] M. Kitazawa, T.R. Yamasaki, F.M. LaFerla, Microglia as a potential bridge between the amyloid beta-peptide and tau, Ann. N. Y. Acad. Sci. 1035 (2004) 85–103.
[18] D. Mattei, A. Djodari-Irani, R. Hadar, A. Pelz, L.F. de Cossío, T. Goetz, M. Matyash, H. Kettenmann, C. Winter, S.A. Wolf, Minocycline rescues decrease in neurogenesis, increase in microglia cytokines and deficits in sensorimotor gating in an animal model of schizophrenia, Brain Behav. Immun. 38 (2014) 175–184.
[19] S. Alawieyah Syed Mortadza, J.A. Sim, V.E. Neubrand, L.H. Jiang, A critical role of TRPM2 channel in $A\beta_{42}$-induced microglial activation and generation of tumor necrosis factor-alpha, Glia 66 (2018) 562–575.
[20] B. Becher, S. Spath, J. Goverman, Cytokine networks in inflammation, Nat. Rev. Immunol. 17 (2017) 49–59.
[21] J. Ji, T. Xue, X. Guo, J. Yang, R. Guo, J. Wang, J. Huang, X. Zhao, X. Sun, Antagonizing peroxisome proliferator-activated receptor γ facilitates M1-to-M2 shift of microglia by enhancing autophagy via the LKB1-AMPK signaling pathway, Aging Cell 17 (2018) e12774.
[22] R. Orihuela, C.A. McPherson, G.J. Harry, Microglial M1/M2 polarization and metabolic states, Brit. J. Pharmacol. 173 (2016) 649–665.
[23] S. Murphy, Production of nitric oxide by glial cells: regulation and potential roles in the CNS, Glia 29 (2000) 1–13.
[24] P.P. Nahar, M.V. Driscoll, L. Li, A.L. Slitt, N.P. Seeram, Phenolic mediated anti-inflammatory properties of a maple syrup extract in RAW 264.7 murine macrophages, J. Funct. Foods. 6 (2014) 126–136.
[25] K.I. Andreasson, A.D. Bachstetter, M. Colonna, F. Ginhoux, C. Holmes, B. Lamb, G. Landreth, D.C. Lee, D. Low, M.A. Lynch, A. Monsonego, M.K. O'Banion, M. Pekny, T. Puschmann, N. Russek-Blum, L.A. Sandusky, M.L. Selenica, K. Takata, J. Teeling, T. Town, L.J. Van Eldik, Targeting innate immunity for neurodegenerative disorders of the central nervous system, J. Neurochem. 138 (2016) 653–693.
[26] C. Tsatsanis, A. Androulidaki, M. Venihaki, A.N. Margioris, Signalling networks regulating cyclooxygenase-2, Int. J. Biochem. Int. J. Biochem. Cell. Biol. 38 (2006) 1654–1661.
[27] M.G. Dilshara, K.T. Lee, R.G. Jayasooriya, C.H. Kang, S.R. Park, Y.H. Choi, I.W. Choi, J.W. Hyun, W.Y. Chang, Y.S. Kim, H.J. Lee, G.Y. Kim, Downregulation of NO and PGE in LPS-stimulated BV2 microglial cells by trans-isoferulic acid via suppression of PI3K/Akt-dependent NF-κB and activation of Nrf2-mediated HO-1, Int. Immunopharmacol. 18 (2014) 203–211.
[28] S. Sil, T. Ghosh, R. Ghosh, P. Gupta, Nitric oxide synthase inhibitor, aminoguanidine reduces intracerebroventricular colchicine induced neurodegeneration, memory impairments and changes of systemic immune responses in rats, J. Neuroimmunol. 303 (2017) 51–61.
[29] I.C. Hoogland, C. Houbolt, D.J. van Westerloo, W.A. van Gool, D. van de Beek, Systemic inflammation and microglial activation: systematic review of animal experiment, J. Inflammation. 12 (2015) 114.
[30] E. Cacci, M.A. Ajmone-Cat, T. Anelli, S. Biagioni, L. Minghetti, In vitro neuronal and glial differentiation from embryonic or adult neural precursor cells are differently affected by chronic or acute activation of microglia, Glia 56 (2008) 412–425.
[31] A. Yan, Z. Liu, L. Song, X. Wang, Y. Zhang, N. Wu, J. Lin, Y. Liu, Z. Liu, Idebenone alleviates inflammation and modulates microglial polarization in LPS-stimulated BV2 cells and MPTP-induced Parkinson's disease mice, Front. Cell. Neurosci. 12 (2019) 529.
[32] X. Hu, P. Li, Y. Guo, H. Wang, R.K. Leak, S. Chen, Y. Gao, J. Chen, Microglia/macrophage polarization dynamics reveal novel mechanism of injury expansion after focal cerebral ischemia, Stroke 43 (2012) 3063–3070.
[33] C. Perego, S. Fumagalli, M.G. De Simoni, Temporal pattern of expression and colocalization of microglia/macrophage phenotype markers following brain ischemic injury in mice, J. Inflammation. 8 (2011) 174.
[34] C.Y. Xia, S. Zhang, Y. Gao, Z.Z. Wang, N.H. Chen, Selective modulation of microglia polarization to M2 phenotype for stroke treatment, Int. Immunopharmacol. 25 (2015) 377–382.
[35] J. Xu, C. Yuan, G. Wang, J. Luo, H. Ma, L. Xu, Y. Mu, Y. Li, N.P. Seeram, X. Huang, L. Li, Urolithins attenuate LPS-induced inflammation in BV2 microglia via MAPK, Akt, and NF-κB signaling pathways, J. Agric. Food Chem. 66 (2018) 571–580.
[36] A. Maqbool, M. Lattke, T. Wirth, B. Baumann, Sustained, neuron-specific IKK/NF-κB activation generates a selective inflammatory response promoting local neurodegeneration with aging, Mol. Neurodegener. 8 (2013) 40.
[37] N.D. Perkins, Integrating cell-signalling pathways with NF-kappaB and IKK function, Nat. Rev. Mol. Cell. Biol. 8 (2007) 49–62.
[38] A. Saccani, T. Schioppa, C. Porta, S.K. Biswas, M. Nebuloni, L. Vago, B. Bottazzi, M.P. Colombo, A. Mantovani, A. Sica, p50 Nuclear factor- B overexpression in tumor-associated macrophages inhibits M1 inflammatory responses and antitumor resistance, Cancer Res. 66 (2006) 11432–11440.
[39] H. Liang, A. Chen, X. Lai, J. Liu, J. Wu, Y. Kang, X. Wang, L. Shao, Inflammation is induced by tongue-instilled ZnO nanoparticles via the Ca^{2+}-dependent NF-κB and MAPK pathways, Part. Fibre Toxicol. 15 (2018) 39.
[40] A. Ghosh, A. Roy, X. Liu, J.H. Kordower, E.J. Mufson, D.M. Hartley, S. Ghosh, R.L. Mosley, H.E. Gendelman, I. Pahant, Selective inhibition of NF-kappaB activation prevents dopaminergic neuronal loss in a mouse model of Parkinson's disease, Proc. Natl. Acad. Sci. U.S.A. 104 (2007) 18754–18759.
[41] E.J. Lee, H.M. Ko, Y.H. Jeong, E.M. Park, H.S. Kim, β-Lapachone suppresses inflammation by modulating the expression of cytokines and matrix

metalloproteinases in activated microglia, J. Inflammation. 12 (2015) 133.
[42] E.K. Kim, E.J. Choi, Compromised MAPK signaling in human diseases: an update, Arch. Toxicol. 89 (2015) 867–882.
[43] M.R. Guimarães, F.R. Leite, L.C. Spolidorio, K.L. Kirkwood, C. Rossa Jr, Curcumin abrogates LPS-induced pro-inflammatory cytokines in RAW 264.7 macrophages. Evidence for novel mechanisms involving SOCS-1, -3 and p38 MAPK, Arch. Oral. Biol. 58 (2013) 1309–1317.
[44] B. Cai, K.J. Seong, S.W. Bae, C. Chun, W.J. Kim, J.Y. Jung, A synthetic diosgenin primary amine derivative attenuates LPS-stimulated inflammation via inhibition of NF-κB and JNK MAPK signaling in microglial BV2 cells, Int. Immunopharmacol. 61 (2018) 204–214.
[45] S. Saccani, S. Pantano, G. Natoli, p38-Dependent marking of inflammatory genes for increased NF-kappa B recruitment, Nat. Immunol. 3 (2002) 69–75.
[46] B. Cai, K.J. Seong, S.W. Bae, M.S. Kook, C. Chun, J.H. Lee, W.S. Choi, J.Y. Jung, W.J. Kim, Water-soluble arginyl–diosgenin analog attenuates hippocampal neurogenesis impairment through blocking microglial activation underlying NF-κB and JNK MAPK signaling in adult mice challenged by LPS, Mol. Neurobiol. (2019), https://doi.org/10.1007/s12035-019-1496-3.